

Functional Diffusion Maps

M. Barroso^{1*}, C.M. Alaíz^{1†}, J.L. Torrecilla^{2†} and A. Fernández^{1†}

^{1*}Departamento de Ingeniería Informática, Universidad Autónoma de Madrid, Spain.

²Departamento de Matemáticas, Universidad Autónoma de Madrid, Spain.

*Corresponding author(s). E-mail(s):

maria.barrosoh@estudiante.uam.es;

Contributing authors: carlos.alaiz@uam.es;

joseluis.torrecilla@uam.es; a.fernandez@uam.es;

†These authors contributed equally to this work.

Abstract

Nowadays many real-world datasets can be considered as functional, in the sense that the processes which generate them are continuous. A fundamental property of this type of data is that in theory they belong to an infinite-dimensional space. Although in practice we usually receive finite observations, they are still high-dimensional and hence dimensionality reduction methods are crucial. In this vein, the main state-of-the-art method for functional data analysis is Functional PCA. Nevertheless, this classic technique assumes that the data lie in a linear manifold, and hence it could have problems when this hypothesis is not fulfilled. In this research, attention has been placed on a non-linear manifold learning method: Diffusion Maps. The article explains how to extend this multivariate method to functional data and compares its behavior against Functional PCA over different simulated and real examples.

Keywords: Unsupervised functional data analysis, Dimensionality reduction methods, Functional diffusion maps, Manifold learning

1 Introduction

In many real-world applications, data must be considered as discretized functions rather than standard vectors, since the process that generates them is assumed to be continuous. Natural examples are found in medicine, economics, speech recognition or meteorological problems. This type of data, commonly called functional data, is usually represented by high-dimensional vectors whose coordinates are highly correlated, and thus multivariate methods lead to ill-conditioned problems. As a consequence, most traditional data analysis tools, such as regression, classification or clustering, are being adapted to functional inputs, as well as some dimensionality reduction techniques.

Functional Data Analysis (FDA; [1]) is an active field of statistics with many close connections to time series analysis, in which the data of interest are realizations of stochastic processes over a compact domain. Originally, FDA focused on linear dimensionality reduction methods, such as Functional Principal Component Analysis (FPCA), and linear models [1], from which numerous applications emerged [2, 3]. In recent years, non-linear functional models have been widely studied, for instance, Functional Support Vector Machines (FSVM; [4]) appeared as a possible non-linear method for data classification, Functional Neural Networks were proposed for regression problems [5] and Functional Isomap [6] emerged as a non-linear dimensionality reduction method based on manifold learning, where an underlying manifold assumption is made over functional data.

Dimensionality reduction methods are statistical techniques where high-dimensional data are represented in lower dimensional spaces, for example by capturing most of the variance of the original data in the new space, like Principal Components Analysis (PCA) [7] does, or by reflecting lower dimensional underlying manifolds where the original data lay, as manifold learning techniques intend [8]. When data are functions, they live in infinite-dimensional spaces, and hence finding low-dimensional representations becomes essential. Finding reliable representations of low-dimensional data, specifically in two or three dimensions, is beneficial in real-world problems for visualization, description and general exploration purposes [9]. Moreover, these representations can be used as feature vectors in supervised machine learning algorithms which require multivariate inputs [10].

The current paper focuses on non-linear dimensionality reduction methods and, in particular, in the manifold learning technique called Diffusion Maps (DM), which we extend to the FDA context by proposing a new method: Functional Diffusion Maps (FDM). As DM, which has been successfully applied in various multivariate [11, 12] and even time-series data [13, 14], FDM has the potential to deliver competitive results in functional data applications, particularly in cases where the data is distributed on specific manifolds. The main contribution of this research can thus be summarized in extending DM to the functional domain, offering a theoretical development, and showing simulated and real examples where FDM outperforms FPCA.

The rest of the paper is organized as follows: Section 2 summarizes some multivariate dimensionality reduction methods, reviewing the general framework for FDA and in particular FPCA as a dimensionality reduction method. Section 3 formalizes the FDM approach and Section 4 illustrates and compares the performance of DM, FPCA, Isomap and FDM on synthetic and real datasets. Finally, Section 5 presents some conclusions of this work, as well as possible research lines to further improve it.

2 FDA and dimensionality reduction methods

As stated above, the focus of this work is on the context of functional data statistics and, in particular, on functional dimensionality reduction methods. In this section, we will introduce the background theory, by first summarizing the main multivariate non-linear dimensionality reduction frameworks. Next, the theoretical framework of FDA is presented, paying special attention to functional manifolds, which will be the main assumption in DM. And finally, FPCA is detailed, which is the main functional dimensionality reduction method in FDA state of the art.

2.1 Overview of multivariate non-linear dimensionality reduction methods

Non-linear dimensionality reduction [9] is based on the assumption that high dimensional data observed in a D -dimensional space \mathbb{R}^D actually lie on (or close to) a d -dimensional manifold $\mathcal{M} \subset \mathbb{R}^D$, with $d < D$ [15]. Manifold learning algorithms often have the property of “unfolding” the manifold where the original data is embedded.

These techniques can be used for discovering high-density low-dimensional surfaces in unsupervised problems, or as a preprocessing step when applying supervised models, being very useful, for example, for data analysis and visualization [16]. Their goal is to achieve a new representation that captures the structure of the data in a few dimensions while preserving the original local information. For doing this, most of these methods rely on the spectral analysis of a similarity matrix of a graph previously constructed over the original data. Another important characteristic of these methods is that they may arrive at a new space where the Euclidean distance between embedded points somehow corresponds to the original information preserved.

Isometric feature mapping (Isomap) [17], t-distributed Stochastic Neighborhood Embedding (t-SNE) [18], Locally Linear Embedding (LLE) [19] or Diffusion Maps (DM) [20, 21] are some of the main manifold methods used for dimensionality reduction over multivariate data. They all take advantage of the local linearity of manifolds and create a mapping that preserves local neighborhoods at each point of the underlying manifold.

2.2 Functional Data Analysis

Functional Data Analysis (FDA) [1, 22, 23] studies samples of random functions $x_1(t), \dots, x_N(t)$, where $t \in \mathcal{J}$, \mathcal{J} is a compact interval, and each $x_i(t)$ is the observation of an independent functional variable X_i identically distributed as X . It is usual to assume that the functional variable X is a second order stochastic process, $E[X^2] < \infty$, and takes values in the Hilbert space of square integrable functions $L^2([a, b])$ defined on the closed interval $[a, b] \subset \mathbb{R}$. The associated inner product for such functions is $\langle x, y \rangle = \int_a^b x(t)y(t)dt$, and the most common type of norm, called L^2 -norm, is related to the above inner product through the relation $\|x\|^2 = \langle x, x \rangle = \int_a^b x^2(t)dt$.

2.2.1 Functional data representation

Although each function x_i consists of infinitely many values $x_i(t)$ with $t \in \mathcal{J}$, in practice we only observe a finite set of function values in a set of arguments that are not necessarily equidistant or equal for all functions [3]. A main problem representing functional data is that we can not directly retrieve the underlying function and we need to work with the functions using specific approaches: working directly with discrete data or transforming it into a function using a basis function expansion. We will briefly sketch below both approaches (for a throughout explanation the reader can refer to [1]).

The first approach is the most common as it consists in using directly the observed values of the functions and it does not require any additional adjustment or assumption. Let $\{x_i(t)\}_{i=1}^N$ be N underlying functions from which we have obtained our data $\mathbf{x}_i = (x_i(t_1), \dots, x_i(t_M))^T$; we denote our set of data as the $N \times M$ matrix defined as

$$\mathbf{X} = \begin{pmatrix} \mathbf{x}_1^T \\ \mathbf{x}_2^T \\ \vdots \\ \mathbf{x}_N^T \end{pmatrix} = \begin{pmatrix} x_1(t_1) & x_1(t_2) & \cdots & x_1(t_M) \\ x_2(t_1) & x_2(t_2) & \cdots & x_2(t_M) \\ \vdots & \vdots & \ddots & \vdots \\ x_N(t_1) & x_N(t_2) & \cdots & x_N(t_M) \end{pmatrix}. \quad (1)$$

The other possible representation is based on a basis function expansion and it is particularly useful for noisy observations. It consists in projecting functions to a finite-dimensional functional subspace. In particular, the functions are expressed as a linear combination of the truncate basis associated to the subspace, i.e. they are expressed in terms of their coordinates $\phi_k(t)$ on the basis of the subspace such that

$$x_i(t) \approx \sum_{k=1}^K c_{ik} \phi_k(t) = \mathbf{c}_i^T \boldsymbol{\phi}(t),$$

where $\boldsymbol{\phi}(t) = (\phi_1(t), \dots, \phi_K(t))^T$ is the vector containing the functions of the truncated basis and $\mathbf{c}_i = (c_{i1}, \dots, c_{iK})^T$ are the coefficients in the new basis.

In this way, the set of N functional data evaluated at time t can be expressed as follows:

$$X(t) = C\phi(t) = \begin{pmatrix} c_{11}^T \\ c_{21}^T \\ \vdots \\ c_{N1}^T \end{pmatrix} \begin{pmatrix} \phi_1(t) \\ \phi_2(t) \\ \vdots \\ \phi_K(t) \end{pmatrix} = \begin{pmatrix} c_{11} & c_{12} & \cdots & c_{1K} \\ c_{21} & c_{22} & \cdots & c_{2K} \\ \vdots & \vdots & \ddots & \vdots \\ c_{N1} & c_{N2} & \cdots & c_{NK} \end{pmatrix} \begin{pmatrix} \phi_1(t) \\ \phi_2(t) \\ \vdots \\ \phi_K(t) \end{pmatrix}, \quad (2)$$

where C is an $N \times K$ matrix.

There are different possible basis, such as Fourier basis, wavelet, B-Spline, polynomial basis, etc. Depending on the data, the choice of basis can be key to capture as much information as possible about the underlying function. For example, if the data are periodic, a Fourier basis will be of interest, while if they are not, the B-Spline basis is a common choice.

2.2.2 Functional manifolds

A functional manifold \mathcal{M} is a differential manifold which is locally diffeomorphic to \mathbb{R}^d [24]. These manifolds are expressed in terms of an atlas consisting of a set of charts $\{(U_\alpha, \varphi_\alpha)\}$, where U_α are open sets covering \mathcal{M} , and $\varphi_\alpha : U_\alpha \rightarrow \mathbb{R}^d$, the coordinate maps, are diffeomorphisms from U_α to open sets of \mathbb{R}^d . These coordinate maps are commonly used to describe the geometry of the manifold.

In the context of FDA, non-linear dimensionality reduction methods uses “simple” functional manifolds [6], which are differential manifolds that are locally isometric to \mathbb{R}^d . These manifolds are characterized by a single chart (U, φ) , where U is an open set covering \mathcal{M} , and the coordinate map $\varphi : U \rightarrow \mathbb{R}^d$ is an isometry from U to an open set of \mathbb{R}^d . A typical example of a “simple” functional manifold is the well-known Swiss roll manifold.

In our research, we will focus on functions in these “simple” functional manifolds, specifically those that belong to $\mathcal{M} \subset L^2([a, b])$, where $[a, b] \subset \mathbb{R}$ is a closed interval. We will use manifold learning methods to approximate φ and understand the inherent structure of the functional data.

2.3 Functional Principal Component Analysis

Functional Principal Component Analysis (FPCA; [1]) is a linear functional dimensionality reduction method that generalizes multivariate Principal Component Analysis (PCA; [7]) to the case where data are functions. In FPCA, the infinite-dimensional random functions are projected onto the lower dimensional subspace generated by the eigenfunctions of the covariance operator.

Let X be a centered square integrable functional variable taking values on $L^2(\mathcal{J})$ and let $x_1(t), \dots, x_N(t)$ be the observations of N independent functional variables X_1, \dots, X_N identically distributed as X . The sample variability is

characterized by the spectral decomposition of the sample covariance operator,

$$\hat{\Gamma}y(t) = \int_{\mathcal{J}} \hat{\sigma}(t, s)y(s)ds,$$

where $\hat{\sigma}(t, s)$ is the sample covariance function of X .

FPCA projects data into the L -dimensional subspace, so that the variance of $\langle \xi_l, X \rangle$ is maximal:

$$\max_{\xi_l \in L^2(\mathcal{J})} \widehat{\text{Var}}[\langle \xi_l, X \rangle] \quad \text{s.t.} \quad \langle \xi_l, \xi_k \rangle = \delta_{lk}, \quad k \leq l, \quad l = 1, \dots, L,$$

or, equivalently,

$$\max_{\xi_l \in L^2(\mathcal{J})} \int_{\mathcal{J}} \int_{\mathcal{J}} \xi_l(s)\hat{\sigma}(s, t)\xi_l(t)dsdt \quad \text{s.t.} \quad \langle \xi_l, \xi_k \rangle = \delta_{lk}, \quad k \leq l, \quad l = 1, \dots, L.$$

The above expression can be simplified by using the sample covariance operator, leading to the alternative formulation:

$$\max_{\xi_l \in L^2(\mathcal{J})} \langle \hat{\Gamma}\xi_l, \xi_l \rangle \quad \text{s.t.} \quad \langle \xi_l, \xi_k \rangle = \delta_{lk}, \quad k \leq l, \quad l = 1, \dots, L.$$

The solutions of this problem are obtained by solving the eigenequation

$$\hat{\Gamma}\xi_l(t) = \lambda_l \xi_l(t), \quad t \in \mathcal{J}, \quad (3)$$

where $\lambda_1 \geq \lambda_2 \geq \dots \geq 0$ are the eigenvalues and ξ_1, ξ_2, \dots are eigenfunctions, which form an orthonormal basis for the space of functions being analyzed. Hence, any function in that space can be expressed as a linear combination of the eigenfunctions.

The eigenfunctions are called *principal component functions* and the random variables $\theta_l = \langle \xi_l, X \rangle = \int \xi_l(t)X(t)dt$ are called *principal component scores* of X into the ξ_l -direction. Thus, the empirical random scores $\hat{\theta}_{li} = \langle \xi_l, x_i \rangle$ for $i = 1, \dots, N$ correspond to the projections of the functional data x_i onto the functional subspace generated by the principal component ξ_l . The l -th eigenvalue λ_l measures the maximum variation of the empirical scores $\hat{\theta}_{l1}, \dots, \hat{\theta}_{lN}$ into the ξ_l -direction:

$$\begin{aligned} \max_{\xi_l \in L^2(\mathcal{J})} \widehat{\text{Var}}[\langle \xi_l, X \rangle] &= \max_{\xi_l \in L^2(\mathcal{J})} \langle \hat{\Gamma}\xi_l, \xi_l \rangle = \max_{\xi_l \in L^2(\mathcal{J})} \langle \lambda_l \xi_l, \xi_l \rangle \\ &= \lambda_l \max_{\xi_l \in L^2(\mathcal{J})} \langle \xi_l, \xi_l \rangle = \lambda_l. \end{aligned}$$

The percentage of total variation τ_l explained by the l -th principal component function is computed as the ratio

$$\tau_l = \frac{\lambda_l}{\sum_{i \geq 1} \lambda_i},$$

and the accumulated ratio of variation τ_L^C explained by the first L principal component functions is computed as

$$\tau_L^C = \frac{\sum_{l=1}^L \lambda_l}{\sum_{i \geq 1} \lambda_i}.$$

Since the amount of explained variation will decline when L increases, we expect that a small number L of components will be sufficient to account for a large part of variation. Indeed, the total approximated error $\sum_{k \geq L+1} \lambda_k$ is expected to be sufficiently small so that $\hat{X}_i = \sum_{l=1}^L \hat{\theta}_{li} \xi_l$ is a good approximation of X_i for a relevant choice of L .

For applying this method there exist two possible strategies to approach the eigenanalysis problem (3). In both cases, we convert the continuous functional eigenanalysis problem to an approximately equivalent matrix eigenanalysis task.

The first strategy consists in discretizing the functions. In this case, FPCA is equivalent to a standard multivariate PCA applied to discrete observed functions X with the metric defined by the quadrature weights matrix. The whole procedure is shown in Algorithm 1.

When functional data are expressed as a linear combination of known basis functions, the eigenequation problem can be reduced to a discrete form expressing the eigenfunctions in the same known basis [25]. This method only differs from the previous one in that the coefficient vectors $\mathbf{b}_l = (b_{l1}, \dots, b_{lK})^\top$ play the role of the vectors of discretized functions $\mathbf{x}_i = (x_i(t_1), \dots, x_i(t_M))^\top$. FPCA is then equivalent to a standard multivariate PCA applied to the matrix of coefficients C with the metric defined by the inner product matrix of the basis. The whole procedure in this case is summarized in Algorithm 2.

3 Functional Diffusion Maps

In this work, we propose a new Functional Manifold Learning technique, which we call Functional Diffusion Maps (FDM), that aims to find low-dimensional representations of L^2 functions on non-linear functional manifolds. It first builds a weighted graph based on pairwise similarities between functional data and then, just like Diffusion Maps (DM) does, uses a diffusion process on the normalised graph to reveal the overall geometric structure of the data at different scales.

Algorithm 1 FPCA - Discretized functions

Input:

- X – Functional data matrix
- L – Embedding dimension
- $\{t_j\}_{j=1}^M$ – Quadrature points

Output:

- $\{\tilde{\xi}_l\}_{l=1}^L$ – Discretized principal component functions
 - $\{\hat{\theta}_l\}_{l=1}^L$ – Principal component scores
- 1: Compute sample covariance matrix $\hat{\Sigma} = N^{-1}X^T X$, where N is the number of functional data.
 - 2: Compute weight matrix W from quadrature weights using some numeric integration rule.
 - 3: Obtain eigenvalues $\{\lambda_l\}_{l=1}^L$ and eigenvectors $\{u_l\}_{l=1}^L$ of $W^{1/2}\hat{\Sigma}W^{1/2}$ satisfying

$$W^{1/2}\hat{\Sigma}W^{1/2}u_l = \lambda_l u_l \quad \text{s.t.} \quad u_l^T u_k = \delta_{lk}, \quad l, k = 1, \dots, L.$$

- 4: Calculate discretized principal component functions $\tilde{\xi}_l = W^{-1/2}u_l$.
 - 5: Calculate principal components scores $\hat{\theta}_l = XW\tilde{\xi}_l$.
-

Even though giving a geometric interpretation of similarity between functional data is sometimes not possible, FDM retains the advantages of multivariate DM as it is robust to noise perturbation. FDM is also a very flexible algorithm that allows fine-tuning of parameters that influence the resulting embedding.

In the following, the theoretical framework for DM is detailed, and then a generalization for functional data is proposed.

3.1 Theoretical framework for Diffusion Maps

DM is a non-linear dimensionality reduction algorithm introduced by Coifman and Lafon [20] which focus on discovering the underlying manifold from which multivariate data have been sample. DM computes a family of embeddings of a dataset into a low-dimensional Euclidean subspace whose coordinates are computed from the eigenvectors and eigenvalues of a diffusion operator on the data.

In particular, let $\mathcal{X} = \{x_1, \dots, x_N\}$ be our multivariate dataset, such that \mathcal{X} is lying along a manifold $\mathcal{M} \subset \mathbb{R}^D$. A random walker will be defined on the data, so the connectivity or similitude between two data points x and y can be used as the probability of walking from x to y in one step of the random walk. Usually, this probability is specified in terms of a kernel function of the two points, $k : \mathbb{R}^D \times \mathbb{R}^D \rightarrow \mathbb{R}$, which has the following properties:

- k is symmetric: $k(x, y) = k(y, x)$;
- k is positivity preserving: $k(x, y) \geq 0 \forall x, y \in \mathcal{X}$.

Algorithm 2 FPCA - Basis function expansion

Input:

- X – Functional data matrix in basis expansions $C\phi$
- L – Embedding dimension

Output:

- $\{\xi_l\}_{l=1}^L$ – Principal component functions
 - $\{\hat{\theta}_l\}_{l=1}^L$ – Principal component scores
- 1: Compute sample covariance matrix of coefficients $\hat{\Sigma}_\phi = N^{-1}C^\top C$, where N is the number of functional data.
 - 2: Compute basis inner product matrix $W = \int \phi^\top \phi$ using some numeric integration rule.
 - 3: Obtain eigenvalues $\{\lambda_l\}_{l=1}^L$ and eigenvectors $\{u_l\}_{l=1}^L$ of $\hat{\Sigma}_\phi$ satisfying

$$W^{1/2}\hat{\Sigma}_\phi W^{1/2}u_l = \lambda_l u_l \quad \text{s.t.} \quad u_l^\top u_k = \delta_{lk}, \quad l, k = 1, \dots, L.$$

- 4: Calculate the coefficients of the principal component functions $b_l = W^{-1/2}u_l$.
 - 5: Calculate principal component functions $\xi_l(t) = b_l^\top \phi(t)$.
 - 6: Calculate principal component scores $\hat{\theta}_l = CWb_l$.
-

Let $G = (\mathcal{X}, K)$ be a weighted graph where K is an $N \times N$ kernel matrix whose components are $k_{ij} = k(x_i, x_j)$. This graph is connected and captures some geometric features of interest in the dataset. Now, to build a random walk, G has to be normalized.

Since the graph depends on both the geometry of the underlying manifold and the data distribution on the manifold, in order to control the influence of the latter, DM uses a density parameter $\alpha \in [0, 1]$ in the normalization step. The normalized graph $G' = (\mathcal{X}, K^{(\alpha)})$ uses the weight matrix $K^{(\alpha)}$ obtained by normalizing K :

$$k_{ij}^{(\alpha)} = \frac{k_{ij}}{d_i^\alpha d_j^\alpha},$$

where $d_i = \sum_{j=1}^N k_{ij}$ is the degree of the graph and the power d_i^α approximates the density of each vertex.

Now, we can create a Markov chain on the normalized graph whose transition matrix P is defined by

$$p_{ij} = \frac{k_{ij}^{(\alpha)}}{d_i^{(\alpha)}},$$

where $d_i^{(\alpha)}$ is the degree of the normalized graph,

$$d_i^{(\alpha)} = \sum_j k_{ij}^{(\alpha)} = \sum_j \frac{k_{ij}}{d_i^\alpha d_j^\alpha}.$$

Each component p_{ij} of the transition matrix P provides the probabilities of arriving from node i to node j in a single step. By taking powers of the P matrix we can increase the number of steps taken in the random walk. Thus, the components of P^T , namely p_{ij}^T , represent the sum of the probabilities of all paths of length T from i to j . This defines a *diffusion process* that reveals the global geometric structure of \mathcal{X} at different scales.

The transition matrix of a Markov chain has a stationary distribution, given by

$$\pi_i = \frac{d_i^{(\alpha)}}{\sum_k d_k^{(\alpha)}},$$

that satisfies the stationary property as follows:

$$\sum_{i=1}^N \pi_i p_{ij} = \sum_{i=1}^N \frac{d_i^{(\alpha)}}{\sum_k d_k^{(\alpha)}} \frac{k_{ij}^{(\alpha)}}{d_i^{(\alpha)}} = \sum_{i=1}^N \frac{k_{ij}^{(\alpha)}}{\sum_k d_k^{(\alpha)}} = \frac{d_j^{(\alpha)}}{\sum_k d_k^{(\alpha)}} = \pi_j.$$

Since the graph is connected, the associated stationary distribution is unique. Moreover, since \mathcal{X} is finite, the chain is ergodic. Another property of the Markov chain is that it is reversible, satisfying

$$\pi_i p_{ij} = \frac{d_i^{(\alpha)}}{\sum_k d_k^{(\alpha)}} \frac{k_{ij}^{(\alpha)}}{d_i^{(\alpha)}} = \frac{k_{ij}^{(\alpha)}}{\sum_k d_k^{(\alpha)}} = \frac{k_{ji}^{(\alpha)}}{\sum_k d_k^{(\alpha)}} = \frac{d_j^{(\alpha)}}{\sum_k d_k^{(\alpha)}} \frac{k_{ji}^{(\alpha)}}{d_j^{(\alpha)}} = \pi_j p_{ji}.$$

Taking into account all these properties, we can now define a diffusion distance D_T based on the geometrical structure of the obtained diffusion process. The metric measures the similarities between data as the connectivity or probability of transition between them. The metric is also robust to noise perturbation, since it is defined as an average of all the paths of length T , such that

$$D_T^2(x_i, x_j) = \|p_i^T - p_j^T\|_{L^2(\frac{1}{\pi})}^2 = \sum_k \frac{(p_{ik}^T - p_{jk}^T)^2}{\pi_k}, \quad (4)$$

where $\|\frac{1}{\pi}\|_{L^2}$ represents the L^2 norm weighted by the stationary distribution π , which takes into account the local data point density. Therefore, T plays the role of a scale parameter and $D_T^2(x_i, x_j)$ will be small if there exist a lot of paths of length T that connect x_i and x_j .

Figure 1 shows a visual example of the diffusion distances and the L^2 distances over the classic Moons dataset, which consists of two half circles interspersed. A spectral color bar has been used, with warm colors indicating nearness between the data and cold colors representing remoteness.

Clearly, Moons data live in a non-linear manifold. In the picture, the distances between the point marked with a star and the rest are displayed. It can be seen that the diffusion distance approximates the distance in the manifold, so that points on the same moon are nearer among them than to points on

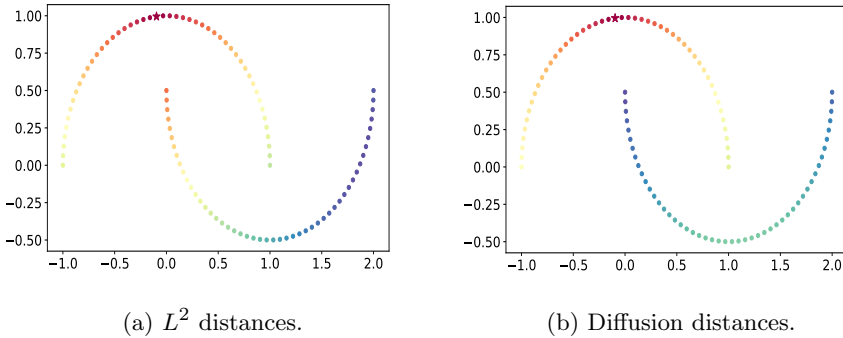


Fig. 1: A comparison between the L^2 distance and the diffusion distance over the Moons dataset.

the other moon. In contrast, L^2 distances are independent of the moons and are not convenient when data live in a non-linear manifold such as this one.

Spectral analysis of the Markov chain allows us to consider an alternative formulation of the diffusion distance that uses eigenvalues and eigenvectors of P .

As detailed in [20], even though P is not symmetric, it makes sense to perform its spectral decomposition using its left and right eigenvectors, such that

$$p_{ij} = \sum_{l \geq 0} \lambda_l (\psi_l)_i (\varphi_l)_j.$$

The eigenvalue $\lambda_0 = 1$ is discarded for P since ψ_0 is a vector with all its values equal to one. The other eigenvalues $\lambda_1, \lambda_2, \dots, \lambda_{N-1}$ tend to 0 and satisfy $\lambda_l < 1$ for all $l \geq 1$. Now, the diffusion distance can be rewritten using the new representation of P :

$$\begin{aligned} D_T^2(x_i, x_j) &= \sum_k \frac{1}{\pi_k} \left(\sum_{l \geq 1} \lambda_l^T (\psi_l)_i (\varphi_l)_k - \sum_{l \geq 1} \lambda_l^T (\psi_l)_j (\varphi_l)_k \right)^2 \\ &= \sum_{l \geq 1} \lambda_l^{2T} ((\psi_l)_i - (\psi_l)_j)^2 \sum_k \frac{(\varphi_l)_k^2}{\pi_k} \\ &= \sum_{l \geq 1} \lambda_l^{2T} ((\psi_l)_i - (\psi_l)_j)^2 \sum_k \frac{((\phi_l)_k \sqrt{\pi_k})^2}{\pi_k} \\ &= \sum_{l \geq 1} \lambda_l^{2T} ((\psi_l)_i - (\psi_l)_j)^2. \end{aligned}$$

Since $\lambda_l \rightarrow 0$ when l grows, the diffusion distance can be approximated using the first L eigenvalues and eigenvectors. One possibility is to select L such that

$$L = \max\{l : \lambda_l^T > \delta \lambda_1^T\},$$

where δ is a parameter that controls the precision in the approximation. Thus, the diffusion distance approximated by L is expressed as

$$D_T^2(x_i, x_j) \approx \sum_{l=1}^L \lambda_l^{2T} ((\psi_l)_i - (\psi_l)_j)^2.$$

Finally, the diffusion map $\Psi_T : \mathcal{X} \rightarrow \mathbb{R}^L$ is defined as

$$\Psi_T(x_i) = \begin{pmatrix} \lambda_1^T \psi_1(x_i) \\ \lambda_2^T \psi_2(x_i) \\ \vdots \\ \lambda_L^T \psi_L(x_i) \end{pmatrix}, \quad (5)$$

With this definition, diffusion maps family $\{\Psi_T\}_{T \in \mathbb{N}}$ projects data points into a Euclidean space \mathbb{R}^L so that diffusion distance on the original space can be approximated by the Euclidean distance of Ψ_T projections in \mathbb{R}^L ,

$$D_T^2(x_i(t), x_j(t)) \approx \sum_{l=1}^L \lambda_l^{2T} ((\psi_l)_i - (\psi_l)_j)^2 = \|\Psi(x_i) - \Psi(x_j)\|^2,$$

preserving the local geometry of the original space.

3.2 Extending Diffusion Maps to functional data

Let X be a centered square integrable functional variable of the Hilbert space $L^2(\mathcal{J})$, where \mathcal{J} is a compact interval. Let $\mathcal{X} = \{x_1(t), \dots, x_N(t)\}$ be the observations of N independent functional variables X_1, \dots, X_N identically distributed as X . We assume that \mathcal{X} lies on a functional manifold $\mathcal{M} \subset L^2(\mathcal{J})$.

Before defining a diffusion process over \mathcal{X} , a random walk over a weighted graph has to be built. Graph vertices are functions $x_i(t) \in \mathcal{X}$ and weights k_{ij} are given by a symmetric positive-definite Kernel operator $\mathcal{K} : L^2(\mathcal{J}) \times L^2(\mathcal{J}) \rightarrow \mathbb{R}$, so that the weight between two vertices $x_i(t)$ and $x_j(t)$ is $k_{ij} = \mathcal{K}(x_i(t), x_j(t))$. Thus, the weighted graph is $G = (\mathcal{X}, K)$, where K is an $N \times N$ kernel matrix resulted from evaluating \mathcal{K} on \mathcal{X} . The kernel operator defines a local measure of similarity within a certain neighborhood, so that outside the neighborhood the function quickly goes to zero. The standard kernel used to compute the similarity between functional data is the Gaussian kernel, which is defined as:

$$\mathcal{K}(x_i(t), x_j(t)) = \exp \frac{-\|x_i(t) - x_j(t)\|_{L^2}^2}{2\sigma^2},$$

where the size of the local neighborhood is determined by the hyperparameter σ . Another classical option is the Laplacian kernel, which is defined as:

$$\mathcal{K}(x_i(t), x_j(t)) = \exp \frac{-\|x_i(t) - x_j(t)\|_{L^1}}{\sigma^2}.$$

These kernels belong to the radial basis function family, which satisfies the property $\mathcal{K}(x(t), y(t)) = \hat{\mathcal{K}}(x(t) - y(t))$, i.e. the kernel only depends on the difference between both elements.

Once the functional data graph G has been constructed, the algorithm performs the same operations as multivariate DM. The full methodology of the method is presented in Algorithm 3.

Algorithm 3 FDM

Input:

- L – Embedding dimension
- T – Steps in random walk
- α – Density parameter
- \mathcal{K} – Kernel operator $\mathcal{K} : L^2(\mathcal{J}) \times L^2(\mathcal{J}) \rightarrow \mathbb{R}$
- $\mathcal{X} = \{x_1(t), \dots, x_N(t)\}$ – Functional data set

Output:

- $\Psi_T(\mathcal{X})$ – Embedded functional data
- 1: Construct $G = (\mathcal{X}, K)$, where K is a positive and symmetric matrix with $k_{ij} = \mathcal{K}(x_i(t), x_j(t))$.
- 2: Compute density of each vertex: $d_i^\alpha = \left(\sum_{j=1}^N k_{ij} \right)^\alpha$.
- 3: Construct $G' = (\mathcal{X}, K^{(\alpha)})$ normalized by α with $k_{ij}^{(\alpha)} = \frac{k_{ij}}{d_i^\alpha d_j^\alpha}$.
- 4: Define transition matrix P with $p_{ij} = \frac{k_{ij}^{(\alpha)}}{d_i^{(\alpha)}}$, where $d_i^{(\alpha)} = \sum_j k_{ij}^{(\alpha)}$.
- 5: Obtain eigenvalues $\{\lambda_l\}_{l \geq 0}$ and right eigenvectors $\{\psi_l\}_{l \geq 0}$ of P such that

$$\begin{cases} 1 & = \lambda_0 > \lambda_1 \geq \dots \\ P\psi_l & = \lambda_l \psi_l. \end{cases}$$

- 6: Calculate diffusion maps

$$\Psi_T(x_i(t)) = \begin{pmatrix} \lambda_1^T \psi_1(x_i(t)) \\ \lambda_2^T \psi_2(x_i(t)) \\ \vdots \\ \lambda_L^T \psi_L(x_i(t)) \end{pmatrix} \quad \forall x_i(t) \in \mathcal{X}.$$

4 Examples and simulation study

In this section we apply the FDM technique described above to synthetic and classic functional datasets. We compare the performance of FDM against its multivariate version and we also evaluate the performance of FDM alongside other FDA techniques, including FPCA and Isomap, to determine its efficacy.

4.1 Cauchy densities data

The purpose of this first experiment is to demonstrate that the straightforward implementation of Diffusion Maps on functional data may not be sufficient if the functions are not equally spaced and the metric employed is unsuitable.

To illustrate this assertion, we apply both DM and FDM in a synthetic example consisting of 50 not equally spaced Cauchy probability density functions with $\gamma = 1.0$. In particular, we generate 25 Cauchy densities with amplitude 1.0 regularly centered in the interval $[-5, 5]$ and 25 Cauchy densities with amplitude 1.5 regularly centered in the same interval. The functions are partitioned into equally spaced sections with 100 data points in each of the following intervals: $[-10, -5]$, $(-5, 5)$, and $[5, 10]$, so that the point density in the middle interval is half that of the other intervals. The functions generated are displayed in Figure 2.

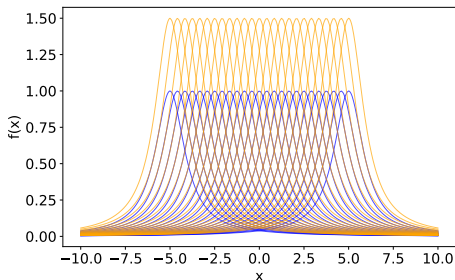


Fig. 2: Cauchy densities data.

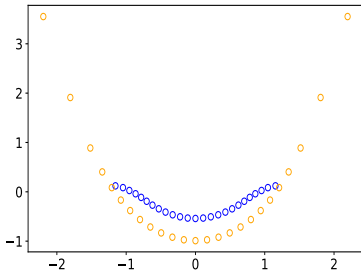
Both DM and FDM require an initial analysis to identify the suitable parameters to cluster the data or reveal the structure of the manifold where the data is supposed to be embedded. To achieve this, a grid search is performed using the hyperparameters specified in Table 1.

After evaluating all possible parameter settings for the Cauchy densities, we found that a Gaussian kernel with a scale parameter of $\sigma = 0.6$ and a density parameter of $\alpha = 1.0$ works better for the DM embedding, while a Gaussian kernel with $\sigma = 0.1$ and $\alpha = 0.0$ is suitable for the FDM technique.

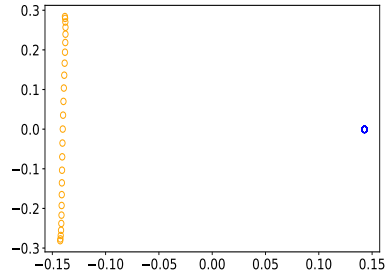
Figure 3 shows the scatterplots of the multivariate and functional scores in the first two components for the Cauchy densities dataset.

Table 1: DM and FDM hyperparameter grids used for finding the best values for the Cauchy densities dataset.

Hyperparam.	Values
α	$\{k/4 : 0 \leq k \leq 4, k \in \mathbb{N}\}$
σ	$\{k/40 : 4 \leq k \leq 8, k \in \mathbb{N}\}$
k	{Gaussian, Laplacian}



(a) DM scores.



(b) FDM scores.

Fig. 3: DM and FDM scores in the first two components for the Cauchy densities dataset.

The DM scores exhibit a semi-circular shape, with the two function classes located in close proximity. In contrast, the FDM scores exhibit a complete separation of function classes. Consequently, we can deduce that the multivariate DM may not be an appropriate method for analyzing non-equispaced functions, for which the functional version of DM provides an essential alternative. The main reason behind this discrepancy lies in the computation of distances.

4.2 Moons and Swiss Roll data

After establishing the necessity of using FDM instead of DM for functional data, we aim to contrast FDM with FPCA by evaluating their performance on the functional versions of the Moons and Swiss Roll datasets.

The Moons dataset shown in Subsection 3.1 is typically used to visualize clustering algorithms. Instead, the Swiss Roll dataset is typically used to test dimensionality reduction techniques. Both of them are common examples where non-linearity in the data makes multivariate PCA perform poorly, and therefore, manifold learning techniques are preferable.

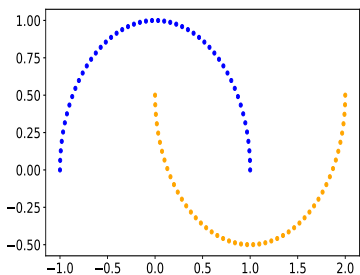
Figure 4 shows, at the left, multivariate Moons and Swiss Roll datasets generated without noise. To get the functional version of these datasets, which are shown in the right panel of Figure 4, the features of multivariate data are used as the coefficient of a chosen functional basis. Specifically, we represent

functional Moons data using the following non-orthogonal basis function:

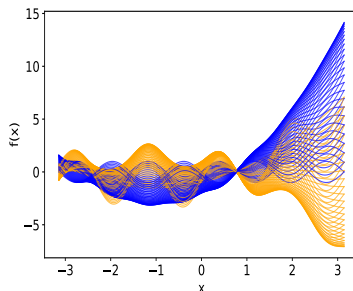
$$\phi(x) = \{\phi_1(x) = \sin(4x), \phi_2 = x^2 + 2x - 2\};$$

for the functional Swiss Roll data we use instead the non-orthogonal basis function:

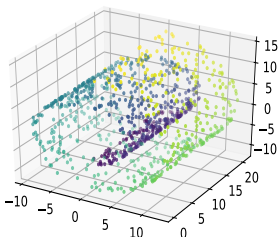
$$\phi(x) = \{\phi_1(x) = \sin(4x), \phi_2 = \cos(8x), \phi_3 = \sin(12x)\}.$$



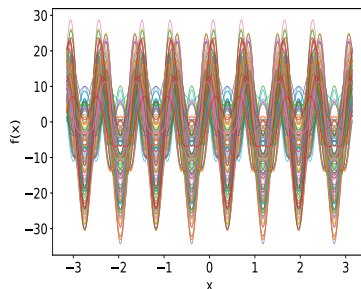
(a) Moons data.



(b) Functional Moons data.



(c) Swiss Roll data.



(d) Functional Swiss Roll data.

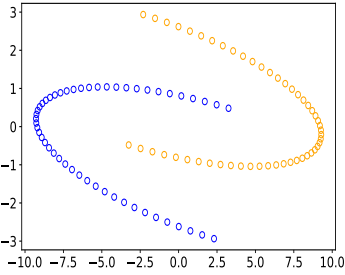
Fig. 4: Left: Multivariate Moons and Swiss Roll data. Right: Functional version of Moons and Swiss Roll data.

Since FPCA and FDM act on the basis function coordinates, we expect to obtain the same results as the multivariate ones, except the effect for the inner product between the chosen basis functions.

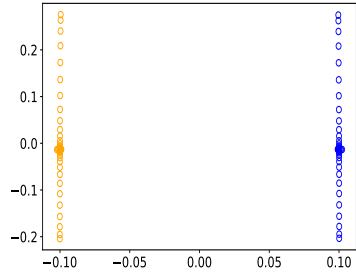
Again, the FDM technique requires an initial analysis to identify suitable parameters. To achieve this, a grid search is performed using the hyperparameters specified in Table 2.

Table 2: FDM hyperparameter grids used for finding the best values for Moons and Swiss Roll datasets.

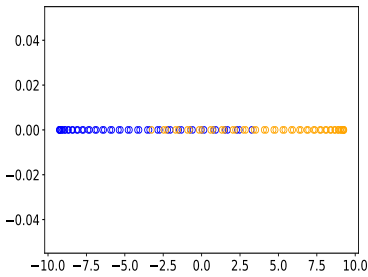
Hyperparam.	Values
α	$\{k/4 : 0 \leq k \leq 4, k \in \mathbb{N}\}$
σ	$\{k/20 : 4 \leq k \leq 8, k \in \mathbb{N}\}$
k	$\{\text{Gaussian, Laplacian}\}$



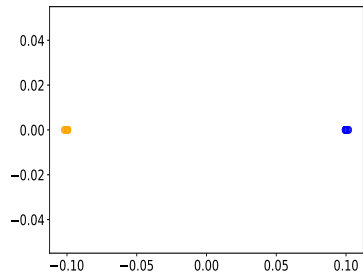
(a) FPCA scores in 2D.



(b) FDM scores in 2D.



(c) FPCA scores projection in 1D.

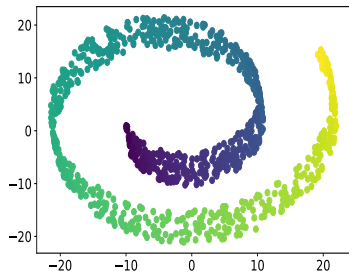


(d) FDM scores projection in 1D.

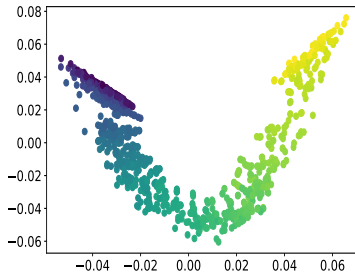
Fig. 5: FPCA and FDM scores for the Moons dataset

After evaluating all possible parameter configurations, we found that a Gaussian kernel with a scale parameter of $\sigma = 0.2$ and a density parameter of $\alpha = 0.5$ works better for the Moons dataset, while a Gaussian kernel with $\sigma = 0.6$ and $\alpha = 1.0$ is more suitable for the Swiss Roll dataset.

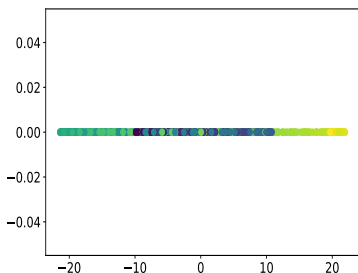
At the top panel of Figures 5 and 6, the Moons and Swiss Roll scatterplots for the FPCA and FDM scores in the first two components are respectively depicted. Furthermore, below the same figures, the projection of the scores in the first component is also presented. These visualizations enable us to discern whether clusters have been recognized or if the underlying manifold has been “unrolled”.



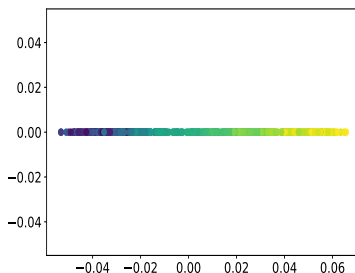
(a) FPCA scores in 2D.



(b) FDM scores in 2D.



(c) FPCA scores projection in 1D.



(d) FDM scores projection in 1D.

Fig. 6: FPCA and FDM scores for the Swiss Roll dataset.

The FPCA embeddings exhibit similarity to the original Moons and Swiss Roll data, with the exception of rotation, sign, and scale adjustments. Instead, the FDM embeddings reveal that Moons data is entirely separated by the first component. Regarding the Swiss Roll, data, the underlying two-dimensional manifold is exposed, and even in one dimension it can be seen that color order is preserved by FDM.

4.3 Phoneme data

In this experiment we have applied the main functional dimensionality reduction techniques—FPCA, Isomap and FDM—to a real dataset, namely the Phoneme dataset, which consists of log-periodograms computed from continuous speech of male speakers for five distinct phonemes. This dataset was extracted from the TIMIT database [26], which is widely used in speech recognition research. The phonemes are transcribed as follows: /sh/ (as in ‘she’), /dcl/ (as in ‘dark’), /iy/ (as the vowel in ‘she’), /aa/ (as the vowel in ‘dark’) and /ao/ (as the first vowel in ‘water’). For our experiment, we take a random

sample of 1500 log-periodograms curves of length 256 as a representative sample of the population due to computational cost. Table 3 shows the phoneme frequencies by class membership.

Table 3: Phoneme frequencies.

aa	ao	dcl	iy	sh
232	358	234	387	289

The log-periodogram curves of the Phoneme dataset are characterized by high irregularity and noise at their endpoints. Hence, in order to prepare them for a dimensionality reduction analysis, a preprocessing step of trimming and smoothing is typically performed. To do this, we truncate the log-periodogram curves to a maximum length of 100, after which we represent them by using a B-Spline basis of order 3 with 9 components.

Figure 7 displays the resulting functional representation of the phoneme dataset.

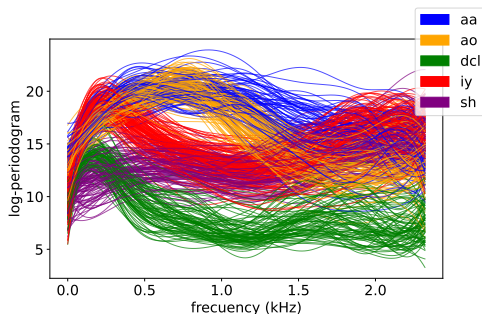


Fig. 7: Phoneme dataset represented by using a B-Spline of order 3 with 9 components.

Looking at the curves, we see higher similarities between the phonemes /aa/ and /ao/, as their sound is very similar; and also between the last part of the curves of phonemes /iy/ and /sh/, since the phoneme /iy/ is contained at the end of the phoneme /sh/. On the other hand, the curves of the phoneme /dcl/ seem to be far away from the rest of the curves.

Next, FPCA, Isomap and FDM are applied to the preprocessed dataset. In this experiment, both Isomap and FDM techniques require an initial analysis to determine the most suitable parameters. To achieve this, we use the same FDM hyperparameter grids from the previous experiment (see Table 2). The Isomap method only requires to set the number of neighbors needed to create the graph. To determine the optimal number of neighbors, we perform a grid search over the set $\{5k : 1 \leq k \leq 5, k \in \mathbb{N}\}$. After evaluating all possible

parameter configurations, we found that a Gaussian kernel with $\sigma = 0.8$ and $\alpha = 1.0$ yields the best results for FDM, while for Isomap, we found that using 10 neighbors provides a suitable performance.

In the left panel of Figure 8, we display the FPCA, Isomap and FDM scores in the first two components for the Phoneme dataset. In the right panel of the same figure, we also present the histograms of the scores associated with the first component. The outcomes yielded by each technique offer different perspectives on phoneme similarities.

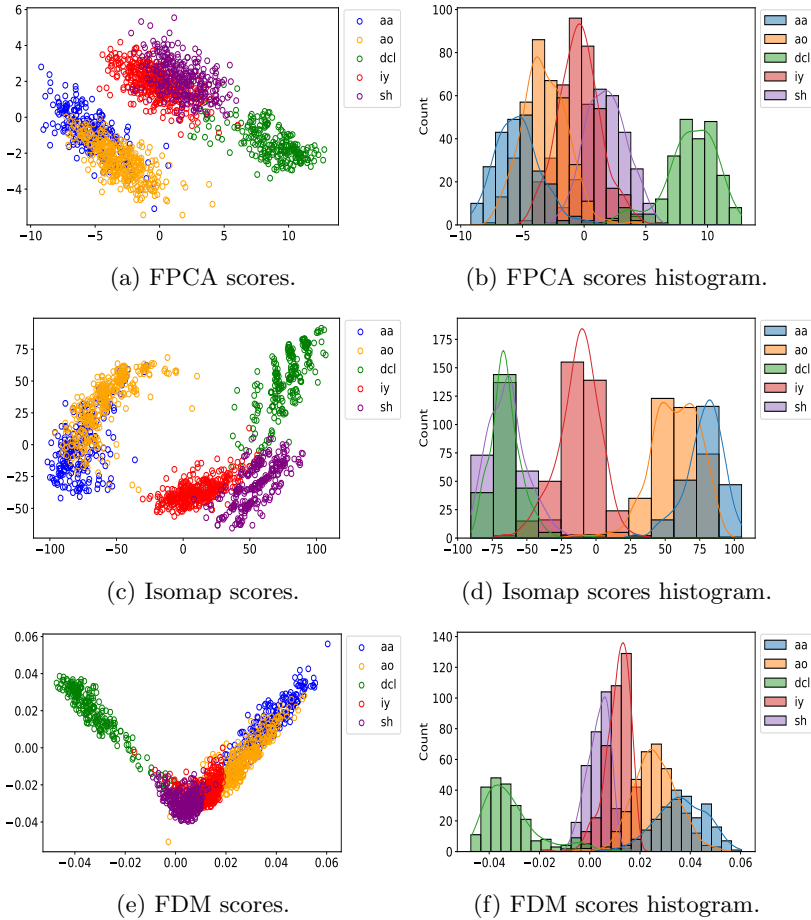


Fig. 8: Left: FPCA, Isomap and FDM scores in the first two components for the Phoneme dataset. Right: FPCA, Isomap and FDM scores histogram in the first component for Phoneme dataset.

FPCA groups each phoneme maintaining the similarities that we had observed from the trajectories. We can also observe in FPCA histogram the

large overlapping between the first component of the phonemes, especially for /ao/, /iy/ and /sh/ phonemes.

Isomap keep similar clusters than FPCA, but without overlapping /iy/ and /sh/ phonemes. Although a more effective separation of /iy/ and /sh/ is observed in the 2D embedding, there is a significant overlap between /dcl/ and /sh/ in the 1D embedding, despite the fact that they should be completely distinct.

FDM embeds the different phoneme groups ordering them from the vowel phonemes (/aa/, /ao/, /iy/) to the word phonemes (/sh/, /dcl/), in the same order as described. In addition, the similarity of the phonemes of the vowel of ‘dark’ (/aa/) and the first vowel of ‘water’ (/ao/) is maintained, appearing close in the embedding, as well as the similarity between the phoneme (/iy/) of the vowel of ‘she’ and the phoneme (/sh/) corresponding to that word. We can also observe that the phoneme of the vowel of ‘she’ (/iy/) is more similar to the phoneme of the first vowel of ‘water’ (/ao/) than to the phoneme of the vowel of ‘dark’, information that we can observe in the curvature of both trajectories. This similarities may be because the phoneme /iy/ is more open than phonemes /ao/ and /iy/ and neither FPCA nor Isomap were able to capture this information.

5 Conclusions

Functional dimensionality reduction methods are statistical techniques that represent infinite-dimensional data in lower dimensional spaces, for example, by capturing most of the variance of the original data in the new space or by reflecting lower dimensional underlying manifolds where the original data lay. Following this second line of research, Diffusion Maps (DM) has been extended to the infinite-dimensional case.

As a result, Functional Diffusion Maps (FDM) emerges as a functional manifold learning technique that finds low-dimensional representations of L^2 functions on non-linear functional manifolds. FDM performs the same operations as DM algorithm once a functional similarity graph is created. Even though giving a geometric interpretation of similarity between functional data is sometimes not possible, FDM retains the advantages of multivariate DM as it is robust to noise perturbation and it is also a very flexible algorithm that allows fine-tuning of parameters that influence the resulting embedding.

The performance of this method has been tested for simulated and real functional examples and the results have been compared with those obtained from the multivariate DM, the linear FPCA method, and the non-linear Isomap technique. It should be noted that the multivariate DM cannot be applied directly to non-equispaced functions, as it may not effectively differentiate the particularities of the functions in study. FDM outperforms FPCA for functions laying in non-linear manifolds such as the Moons and the Swiss Roll examples, where FDM obtains a representation that maintains the original structure of the manifold. Besides being an advantage for these

simulated examples, it also provides good results and allows new similarity interpretations for real examples such as the Phoneme dataset.

Overall, we find that the proposed manifold FDM method is an interesting technique that can provide useful representations which are competitive with, and often superior to, some classical linear and non-linear representations for functional data.

References

- [1] Ramsay, J.O., Silverman, B.W.: *Functional Data Analysis*. Springer, New York (2005)
- [2] Ullah, S., Finch, C.: Applications of functional data analysis: A systematic review. *BMC medical research methodology* **13**, 43 (2013). <https://doi.org/10.1186/1471-2288-13-43>
- [3] Nicol, F.: Functional principal component analysis of aircraft trajectories, 17 (2013)
- [4] Rossi, F., Villa, N.: Support vector machine for functional data classification. *Neurocomputing* **69**(7), 730–742 (2006). <https://doi.org/10.1016/j.neucom.2005.12.010>
- [5] Rao, A.R., Reimherr, M.: Non-linear functional modeling using neural networks. *Journal of Computational and Graphical Statistics* **0**, 1–20 (2023). <https://doi.org/10.1080/10618600.2023.2165498>
- [6] Chen, D., Müller, H.-G.: Nonlinear manifold representations for functional data. *The Annals of Statistics* **40**(1) (2012). <https://doi.org/10.1214/11-aos936>
- [7] Bishop, C.M.: *Pattern Recognition and Machine Learning (Information Science and Statistics)*. Springer, Berlin, Heidelberg (2007)
- [8] Cayton, L.: Algorithms for manifold learning. Univ. of California at San Diego Tech. Rep **12**(1-17), 1 (2005)
- [9] Herrmann, M., Scheipl, F.: Unsupervised Functional Data Analysis via Nonlinear Dimension Reduction. arXiv (2020). <https://doi.org/10.48550/ARXIV.2012.11987>
- [10] Pfisterer, F., Beggel, L., Sun, X., Scheipl, F., Bischl, B.: Benchmarking time series classification – Functional data vs machine learning approaches. arXiv (2019). <https://doi.org/10.48550/ARXIV.1911.07511>
- [11] Fernández, Á., González, A.M., Díaz, J., Dorronsoro, J.R.: Diffusion maps for the description of meteorological data. In: Corchado, E., Snášel, V.,

- Abraham, A., Woźniak, M., Graña, M., Cho, S.-B. (eds.) Hybrid Artificial Intelligent Systems, pp. 276–287. Springer, Berlin, Heidelberg (2012)
- [12] Dov, D., Talmon, R., Cohen, I.: Audio-visual voice activity detection using diffusion maps. *IEEE/ACM Transactions on Audio, Speech, and Language Processing* **23**(4), 732–745 (2015). <https://doi.org/10.1109/TASLP.2015.2405481>
- [13] Marshall, N.F., Hirn, M.J.: Time coupled diffusion maps. *Applied and Computational Harmonic Analysis* **45**(3), 709–728 (2018). <https://doi.org/10.1016/j.acha.2017.11.003>
- [14] Lian, W., Talmon, R., Zaveri, H., Carin, L., Coifman, R.: Multivariate time-series analysis and diffusion maps. *Signal Processing* **116**, 13–28 (2015). <https://doi.org/10.1016/j.sigpro.2015.04.003>
- [15] Cayton, L.: Algorithms for manifold learning (2005)
- [16] Bengio, Y., Delalleau, O., Le Roux, N., Paiement, J.-F., Vincent, P., Ouimet, M.: Spectral Dimensionality Reduction. Springer, Canada (2006)
- [17] Tenenbaum, J.B., de Silva, V., Langford, J.C.: A global geometric framework for nonlinear dimensionality reduction. *Science* **290**(5500), 2319–2323 (2000). <https://doi.org/10.1126/science.290.5500.2319>
- [18] Cox, M.A.A., Cox, T.F.: Multidimensional Scaling, pp. 315–347. Springer, Berlin, Heidelberg (2008). https://doi.org/10.1007/978-3-540-33037-0_14
- [19] Saul, L.K., Roweis, S.T.: An introduction to locally linear embedding. (2001)
- [20] Coifman, R.R., Lafon, S.: Diffusion maps. *Applied and Computational Harmonic Analysis* **21**(1), 5–30 (2006). <https://doi.org/10.1016/j.acha.2006.04.006>
- [21] De la Porte, J., Herbst, B., Hereman, W., Van Der Walt, S.: An introduction to diffusion maps. In: Proceedings of the 19th Symposium of the Pattern Recognition Association of South Africa (PRASA 2008), Cape Town, South Africa, pp. 15–25 (2008)
- [22] Kokoszka, P., Reimherr, M.: Introduction to Functional Data Analysis. Chapman & Hall / CRC numerical analysis and scientific computing. CRC Press, New York (2017)
- [23] Ferraty, F., Vieu, P.: Nonparametric Functional Data Analysis: Theory and Practice. Springer, New York (2006)
- [24] Lee, J.M.: Introduction to smooth manifolds (2000)

- [25] Houzel, C.: Frédéric Riesz et l'Analyse Fonctionnelle (2015). <https://doi.org/10.13140/RG.2.1.2667.1203>
- [26] Garofolo, J.S., Lamel, L.F., Fisher, W.M., Fiscus, J.G., Pallett, D.S., Dahlgren, N.L.: DARPA TIMIT Acoustic Phonetic Continuous Speech Corpus CDROM. NIST (1993)